Conformational Changes of Transfer Ribonucleic Acid. Comparison of the Early Melting Transition of Two Tyrosine-Specific Transfer Ribonucleic Acids

S. K. Yang and D. M. Crothers*

ABSTRACT: The early melting transitions of $tRNA_I^{Tyr}$ and $tRNA_{II}^{Tyr}$ (both from *Escherichia coli*) show remarkably different kinetic properties, and both contrast with $tRNA^{fMet}$ (*E. coli*) as reported by Cole and Crothers (*Biochemistry 11*, 4368 (1972)). In $tRNA_I^{Tyr}$ the early transition is dominated by a single relaxation time, which is much slower than the two relaxation times of $tRNA^{fMet}$. Furthermore, the reaction that leads to formation of the "native" (low temperature) structure has appreciable activation energy (~20 kcal/mole) in contrast to the negligible activation energy for the same process in $tRNA^{fMet}$. The dependence of the rate constants on salt concentration was studied, with the conclusion that addition of salt stabilizes the "native" structure mainly because it slows down the rate of melting (at constant temperature). The melting curve of $tRNA_{II}^{Tyr}$ has a transition not evident in $tRNA_I^{Tyr}$. This "extra" melting step occurs after the early transition, and we conclude that $tRNA_{II}^{Tyr}$ can form a bonded structure not possible for $tRNA_I^{Tyr}$. Furthermore, $tRNA_{II}^{Tyr}$ exhibits two relaxation times in the early transition. The temperature dependence of these two relaxation effects indicates that the slower process in reforming the native structure has appreciable activation energy (>20 kcal/mole), while the faster process has negligible activation energy. The following model accounts for these observations: $tRNA_I^{Tyr}$ and $tRNA_{II}^{Tyr}$ differ by two nucleotides in the variable-length sequence region. In $tRNA_I^{Tyr}$ four nucleotides from that region are complementary to the TψC loop, and bond accordingly after the tertiary structure is melted. This "incorrect" structure blocks formation of the "native" structure and must first be melted, accounting for the slow rate and appreciable activation energy. In $tRNA_{II}^{Tyr}$ the same sequence region is instead complementary to the anticodon loop. This "incorrect" structure (again formed *after* melting of the tertiary structure) is more stable in $tRNA_{II}^{Tyr}$ than in $tRNA_I^{Tyr}$, accounting for the distinct "extra" transition in $tRNA_{II}^{Tyr}$. The bonding between the anticodon loop and the variable-length region blocks only one of the two regions of interaction in the tertiary structure of $tRNA_{II}^{Tyr}$. We find no evidence that the tertiary structure itself is different for the two tRNAs. We suggest the possibility that these conformational differences may be functionally important. If the tertiary structure of tRNA is modified or dissociated during its function, the two tyrosine-specific tRNAs would have different conformations available, corresponding to the two different "incorrect" structures. Thus the variable-length region could affect function by modulating tRNA conformation.

A biochemical problem of considerable current interest is the functional significance of different tRNA molecules that accept the same amino acid. A good example in which the two tRNAs have the same anticodon is provided by the species $tRNA_I^{Tyr}$ and $tRNA_{II}^{Tyr}$ (both from *Escherichia coli*), which differ by two nucleotides in a nonbonded region of the cloverleaf structure (Figure 1). One way these two molecules could differ is in conformational properties, if the base changes provide to one species a bonded structure not available to the other. We shall show that this is the case for $tRNA_I^{Tyr}$ and $tRNA_{II}^{Tyr}$, if conditions are appropriately adjusted.

Also of interest is the contrast between the melting properties of $tRNA^{Tyr}$ and other tRNAs, especially $tRNA^{fMet}$ (*E. coli*) whose melting kinetics we reported in detail in the previous paper in this series (Cole and Crothers, 1972). In particular, we find invalid for $tRNA^{Tyr}$ the conclusion reached for $tRNA^{fMet}$ that no appreciable noncloverleaf bonding is present in zone II of the phase diagram (Cole *et al.*, 1972), which is the conformation present after melting of the tertiary structure. Fortunately, it turns out that the nature of this residual noncloverleaf bonding is clearly different for $tRNA_I^{Tyr}$ and $tRNA_{II}^{Tyr}$. This allows us to conclude that it must involve the sequence region which is different in the two, and leads to a simple model for the source of the bonding.

Materials and Methods

Buffers. Samples for kinetic and equilibrium measurements were dissolved in PCEP buffer (Cole *et al.*, 1972), at Na^+ concentrations of 0.12 M 0.174 M, and 0.5 M.

tRNA Samples. $tRNA^{Tyr}$ was prepared as described previously (Yang, 1972; Cole *et al.*, 1972). Following chromatography on benzoylated DEAE-cellulose (pH 5, ethanol gradient, and again at pH 7.5, NaCl gradient), the tyrosine-specific fractions were pooled. $tRNA_I^{Tyr}$ and $tRNA_{II}^{Tyr}$ were separated on a DEAE-Sephadex A50 column (2 × 170 cm), using a linear NaCl gradient from 0.4 M to 0.47 M, with 0.01 M $MgCl_2$, 0.05% NaN_3, and 0.02 M Tris-HCl, pH 7.5. The first peak ($tRNA_I^{Tyr}$) was rechromatographed for better purity. The acceptor activities were 1550–1650 pmoles/A_{260} unit for $tRNA_I^{Tyr}$ and 1620 pmoles/A_{260} unit for $tRNA_{II}^{Tyr}$.

Melting curves were measured as described previously (Cole *et al.*, 1972).

Temperature-jump measurements were also done as described previously (Yang, 1972; Cole and Crothers, 1972). Precautions were taken to limit the extent of photochemical degradation, and results were checked frequently with fresh

---

† From the Department of Chemistry, Yale University, New Haven, Connecticut 06520. *Received June 9, 1972.* This is the third paper in a series; the preceding paper was by Cole and Crothers (1972). This work was supported by a grant (GM 12589) from the National Institutes of Health. D. M. C. holds a Career Development award (GM 19978) from the same source.

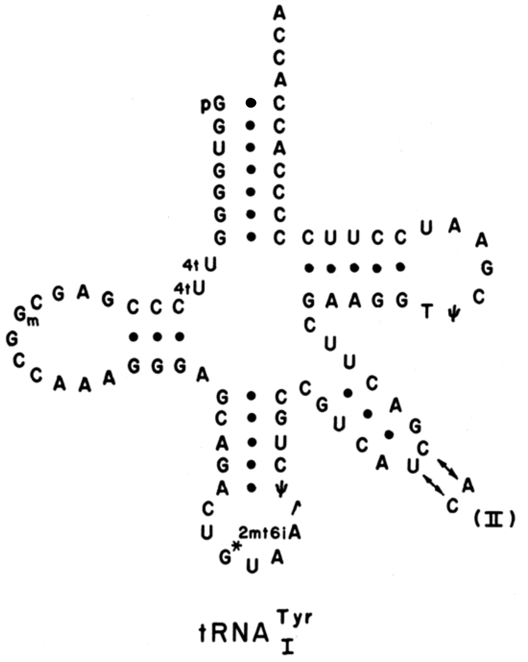

FIGURE 1: Primary structure of *E. coli* tRNA$_{\mathrm{I}}^{\mathrm{Tyr}}$ and tRNA$_{\mathrm{II}}^{\mathrm{Tyr}}$ determined by Goodman *et al.* (1968) and RajBandary *et al.* (1969).

samples to insure that measurements were reproducible. Exposure to the temperature jump itself caused no detectable degradation of tRNA.

Results

Relaxation Kinetics of the Early Melting Transition of tRNA$_I^{Tyr}$ Contrasts Sharply with the Results on tRNA^{fMet}. We investigated the melting kinetics of tRNA$_{\mathrm{I}}^{\mathrm{Tyr}}$ at three different salt concentrations: 0.12 PCEP, 0.174 PCEP, and 0.5 PCEP. Technical difficulties limit the range of measurement in each case, since the relaxation becomes too slow to measure (~1 sec) in the temperature-jump apparatus at low temperature and lower salt concentration (0.12 M and 0.17 M Na$^+$), whereas at higher salt (0.5 M Na$^+$) the dimerization process (Yang *et al.*, 1972) is a serious complication in the high-temperature range. In the latter case, samples could be held at high temperature only for a period short enough to make dimerization negligible. Relaxation times were measured at both 335 and 266 nm, and identical decay times were found within 10% error; relaxation times were independent of tRNA concentration. The major observations of tRNA$_{\mathrm{I}}^{\mathrm{Tyr}}$, which clearly differ from those for tRNA$^{\mathrm{fMet}}$ reported by Cole and Crothers (1972), are summarized in the following paragraphs.

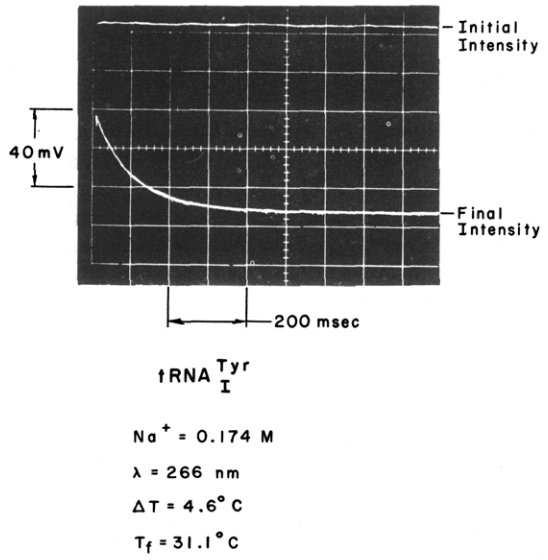

FIGURE 2: Relaxation signal of tRNA$_{\mathrm{I}}^{\mathrm{Tyr}}$ measured in 0.174 PCEP at 266 nm. The temperature jump was 4.6° and the final temperature was 31.1°. The concentration of tRNA$_{\mathrm{I}}^{\mathrm{Tyr}}$ was 0.909 $A_{260}{}^{20°}$/ml. Changes in light intensity ΔI are measured in millivolts; the total intensity is 5 V.

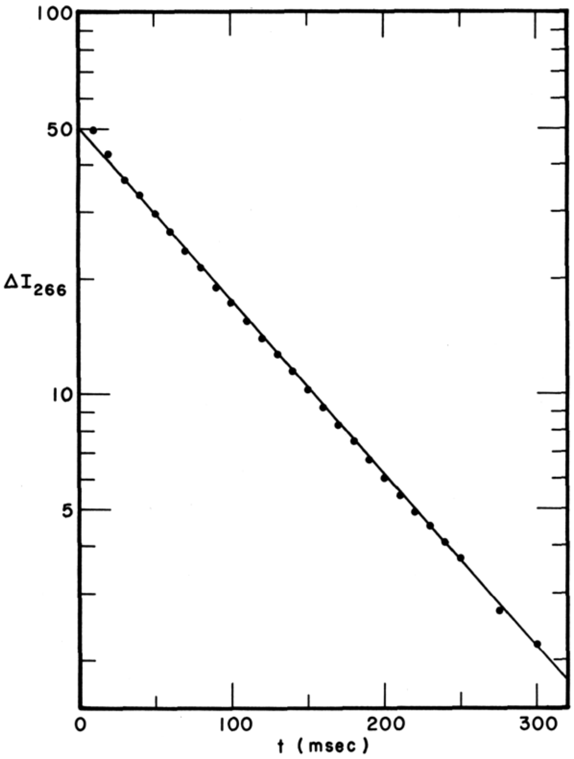

FIGURE 3: Semi-logarithmic plot of the relaxation effect in Figure 2.

The Process Is Dominated by a Single Relaxation Time. In the case of tRNA$^{\mathrm{fMet}}$, two relaxations in the millisecond time range were responsible for most of the kinetic signal. For tRNA$_{\mathrm{I}}^{\mathrm{Tyr}}$ the comparable effect is, to a first approximation, a single relaxation with a time constant that varies from one to hundreds of milliseconds depending on temperature and salt concentration. Figures 2 and 3 show a typical relaxation signal and semi-logarithmic plot of the data. This relaxation effect when measured at 266 nm constitutes 20–70% of the total optical change, and 50–80% of that measured at 335 nm, varying with salt concentration and temperature.

In spite of the single dominant relaxation effect, it is clear that other processes are also occurring in this temperature range. On the very fast time scale there is a relaxation of roughly 30 μsec, which is too small and rapid to measure accurately, as well as an even faster optical change. Approximately 30 μsec is the time range expected for relaxation in the early melting of the dihydrouridine helix, but we have no further evidence to substantiate this assignment. As we will see later, other factors point to the existence of still another small relaxation in the millisecond time range, and we will

TABLE I: Activation Energies (kcal/mole) for the Recombination and Dissociation of $\text{tRNA}_\text{I}^\text{Tyr}$ Tertiary Structure in Neutral Solutions of Three Na^+ Concentrations.[a]

	E_act^R	E_act^D
0.5 PCEP	~24	45
0.174 PCEP		57
0.12 PCEP		62

[a] See Materials and Methods for the description of the buffer system.

subsequently show that it can be extracted from the data.

The Dominant Relaxation Is Much Slower than for $tRNA^{fMet}$, and Has a Different Temperature Dependence. Figure 4 shows the temperature dependence of τ at three salt concentrations. At comparable ionic conditions, the relaxation is 40 times slower at the midpoint than the slower of the two effects in tRNA^fMet at its midpoint (the temperature of maximum amplitude). Furthermore, for $\text{tRNA}_\text{I}^\text{Tyr}$ the relaxation time is not independent of temperature at the lowest temperatures that it can be measured, again in contrast to tRNA^fMet.

Assuming a single dominant relaxation effect, the melting transition may be approximated by

$$\text{N} \underset{k_\text{R}}{\overset{k_\text{D}}{\rightleftharpoons}} \text{II} \tag{1}$$

where N is the "native" (low temperature) form, and II the product of the early melting transition. For this mechanism,

$$1/\tau = k_\text{R} + k_\text{D} \tag{2}$$

At the beginning of the transition, $k_\text{R} \gg k_\text{D}$, and $1/\tau \approx k_\text{R}$, while at the end of melting $k_\text{D} \gg k_\text{R}$ and $1/\tau \approx k_\text{D}$. Hence the Arrhenius activation energies E_act,

$$(\partial \ln k/\partial(1/T))_\text{P} = -E_\text{act}/R \tag{3}$$

can be estimated from the initial and final slopes of a plot of log τ *vs.* $1/T$, as in Figure 4. Table I lists activation parameters determined in this way. The recombination activation energy E_act^R can be estimated only roughly, but it is clear that *there is a substantial positive activation energy for reforming the native structure from form II.*

Dependence of the Kinetic Parameters on Salt Concentration. The variation with salt concentration of τ_m, the value of τ at T_m, can be used to estimate the dependence of k_R and k_D on Na^+ concentration at constant temperature. We note that at T_m, $k_\text{R} = k_\text{D}$ (since the equilibrium constant is one), and let k_m be the value of k_R or k_D at that point. The differential of k_m may be expressed in terms of the variables $[Na^+]$ (sodium ion concentration) and T_m

$$\text{d} \ln k_\text{m} = \left(\frac{\partial \ln k_\text{m}}{\partial(1/T_\text{m})}\right)_{[Na^+]} \text{d}(1/T_\text{m}) + \left(\frac{\partial \ln k_\text{m}}{\partial \ln [Na^+]}\right)_T \text{d} \ln [Na^+] \tag{4}$$

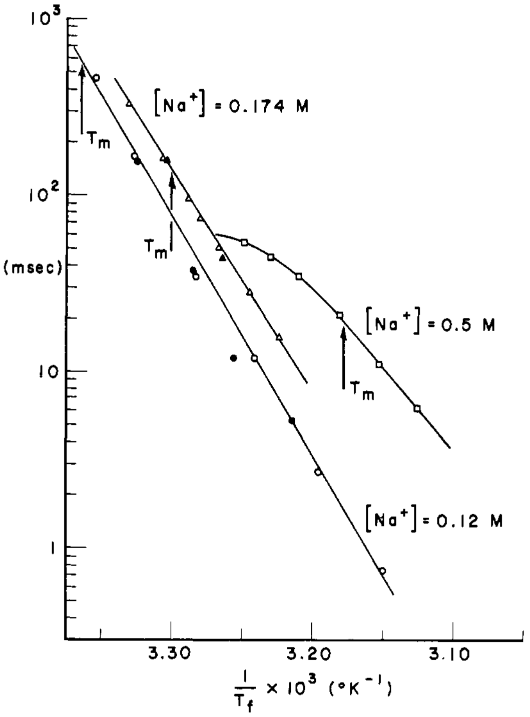

FIGURE 4: Relaxation times of $\text{tRNA}_\text{I}^\text{Tyr}$ determined at 266 (open circles, triangles, and squares) and 335 nm (filled circles and triangles) in 0.12, 0.174, and 0.5 PCEP buffers are plotted *vs.* reciprocal temperatures. T_m values of the thermal transitions are indicated by arrows on the temperature axis. The temperature jump was 4.6° and T_f is the final temperature after the temperature jump.

Hence

$$\frac{\text{d} \ln k_\text{m}}{\text{d} \ln [Na^+]} = \left(\frac{\partial \ln k_\text{m}}{\partial(1/T_\text{m})}\right)_{[Na^+]} \frac{\text{d}(1/T_\text{m})}{\text{d} \ln [Na^+]} + \left(\frac{\partial \ln k_\text{m}}{\partial \ln [Na^+]}\right)_T \tag{5}$$

Using eq 2 and 3 and rearranging yields

$$\left(\frac{\partial \ln k_\text{D}}{\partial \ln [Na^+]}\right)_T = \frac{-\text{d} \ln \tau_\text{m}}{\text{d} \ln [Na^+]} + \frac{E_\text{act}^\text{D}}{R}\left(\frac{\text{d}(1/T_\text{m})}{\text{d} \ln [Na^+]}\right) \tag{6}$$

and a corresponding equation for k_R. Both terms on the right of eq 6 are experimentally accessible; Figure 5 shows the relevant plot. Using 57 kcal/mole for the activation energy of k_D, we obtain

$$\left(\frac{\partial \ln k_\text{D}}{\partial \ln [Na^+]}\right)_T \approx -2.5$$

and, with 24 kcal/mole for the activation energy of k_R,

$$\left(\frac{\partial \ln k_\text{R}}{\partial \ln [Na^+]}\right)_T \approx 0$$

Hence the early melting transition is increased in temperature by higher salt concentration because the rate of dissociation of the native structure is slowed (at constant temperature). The rate of reforming the native structure is nearly independent of salt concentration (at constant temperature).

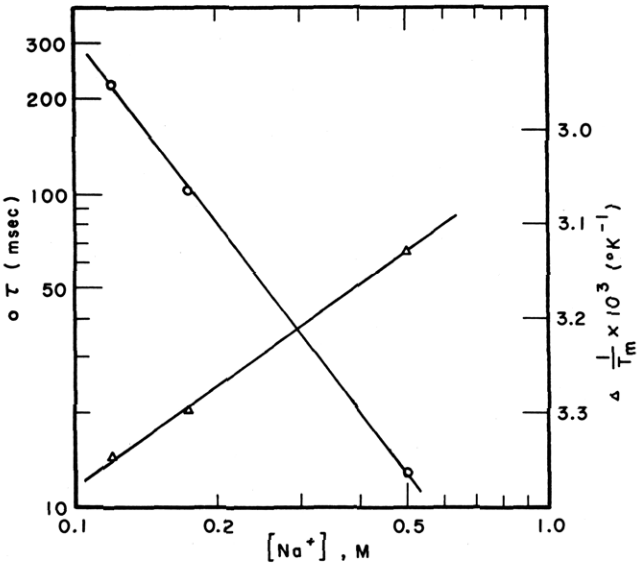

FIGURE 5: Logarithms of $\tau_{\rm m}$ (left axis, data from Figure 4) are plotted *vs.* logarithms of Na$^+$ concentrations, and reciprocal $T_{\rm m}$ values (right axis, data from the phase diagram of tRNA$_{\rm I}^{\rm Tyr}$, Cole *et al.*, 1972), are plotted *vs.* logarithms of Na$^+$ concentrations. The slopes determined from this figure are: $d \ln \tau_{\rm m}/d \ln {\rm Na}^+ = -1.77$, $d(1/T_{\rm m})/d \ln {\rm Na}^+ = 1.5 \times 10^{-4}$.

Comparison of tRNA$_{I}^{Tyr}$ and tRNA$_{II}^{Tyr}$. The results reported so far indicate that reformation of the native structure of tRNA$_{\rm I}^{\rm Tyr}$ from form II occurs against an appreciable activation energy barrier, and is considerably slower than the corresponding reaction of tRNA$^{\rm fMet}$. It therefore seems likely that there is some "incorrect" structure in form II: presumably noncloverleaf bonding that is incompatible with the native structure. In the absence of further information, however, one could only guess at the nature of that bonding. We were fortunate, therefore, to find that the incorrect structure is definitely different in tRNA$_{\rm II}^{\rm Tyr}$, and hence probably involves the sequence region where the two tRNAs differ. This greatly simplifies the problem of developing a structural model for the phenomenon.

The Equilibrium Melting Curve of tRNA$_{II}^{Tyr}$ Shows a Transition Not Evident in tRNA$_{I}^{Tyr}$. Figure 6 shows comparisons of melting curves of tRNA$_{\rm I}^{\rm Tyr}$ and tRNA$_{\rm II}^{\rm Tyr}$ at 260 and 335 nm. At both wavelengths tRNA$_{\rm II}^{\rm Tyr}$ shows indications of a transition centered around ~44°, a transition not evidently present in tRNA$_{\rm I}^{\rm Tyr}$.

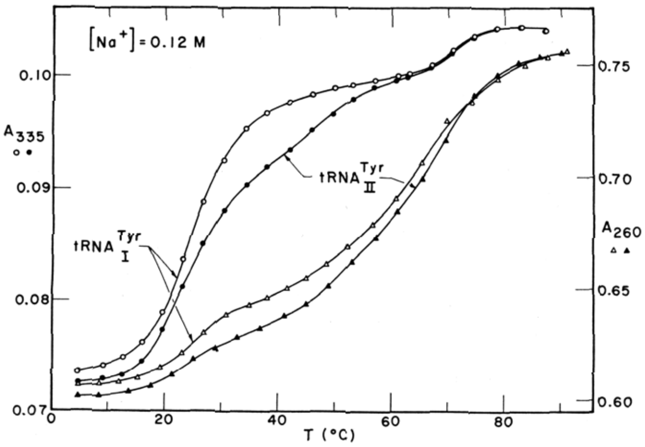

FIGURE 6: Melting curves of tRNA$_{\rm I}^{\rm Tyr}$ and tRNA$_{\rm II}^{\rm Tyr}$ in 0.12 PCEP at 260 (right axis) and 335 nm (left axis).

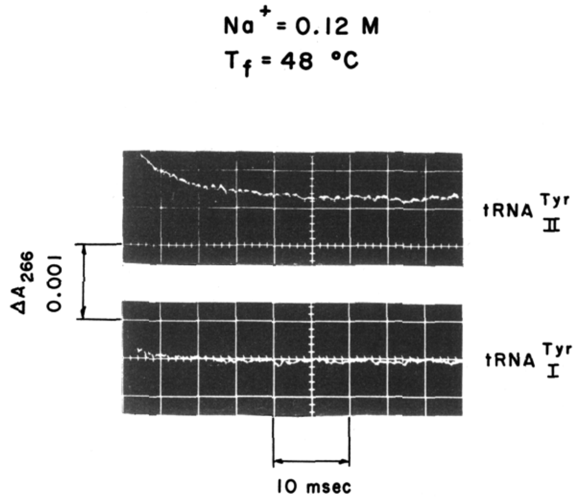

FIGURE 7: Oscilloscope traces of the relaxation signal at 266 nm which is present for tRNA$_{\rm II}^{\rm Tyr}$ and absent for tRNA$_{\rm I}^{\rm Tyr}$ at identical conditions. Both are measured in 0.12 PCEP and have the same final temperatures (48°).

This extra transition may be domonstrated kinetically. Figure 7 shows a comparison of identical temperature-jump experiments on the two tRNAs, taken in the region of the "extra" transition. tRNA$_{\rm II}^{\rm Tyr}$ has a well-defined relaxation with a decay time of about 5 msec, while the kinetic curve for tRNA$_{\rm I}^{\rm Tyr}$ is nearly flat on the same time scale. (Both tRNAs show a very fast optical change at the wavelength of measurement, 266 nm.) We conclude that *after the early melting transition, tRNA$_{II}^{Tyr}$ can form a bonded structure not possible for tRNA$_{I}^{Tyr}$.*

The relaxation kinetics of the early melting transition is very different for tRNA$_{\rm II}^{\rm Tyr}$ than for tRNA$_{\rm I}^{\rm Tyr}$. If the "extra" structure formed by tRNA$_{\rm II}^{\rm Tyr}$ is in some way not compatible with the native tertiary structure, one expects an appreciable activation energy for reforming that structure, and possibly a totally different relaxation pattern than found for tRNA$_{\rm I}^{\rm Tyr}$. Figure 8 demonstrates that this is the case. *tRNA$_{II}^{Tyr}$ exhibits two relaxation times in the early transition, in contrast to the predominantly single relaxation for tRNA$_{I}^{Tyr}$ under identical conditions.*

At this stage in the experiments we reasoned that, since tRNA$_{\rm I}^{\rm Tyr}$ has appreciable activation energy for reforming the native structure, it must also show, at some temperature, a kinetic effect due to melting of the incorrect structure. That is, there must be some relaxation signal analogous to that in Figure 7 for the "extra" transition in tRNA$_{\rm II}^{\rm Tyr}$. Close examination of the data revealed the effect labeled τ_1 in Figure 8. It is reproducibly present and comparable in time scale and amplitude to the signal for tRNA$_{\rm II}^{\rm Tyr}$ in Figure 7. The reason we did not detect it immediately is that it occurs in the same temperature range as the optically more significant dominant relaxation effect. We are therefore now able to report multiple relaxation times for both tRNAs, although Figure 8 makes evident that the distribution of relaxation amplitudes between fast and slow effects is very different for the two tRNAs.

The Slower of the Two tRNA$_{II}^{Tyr}$ Relaxation Times Is Strongly Temperature Dependent at Low Temperature, while the Faster Is Not. Figure 9 shows data at 0.5 M Na$^+$ for both

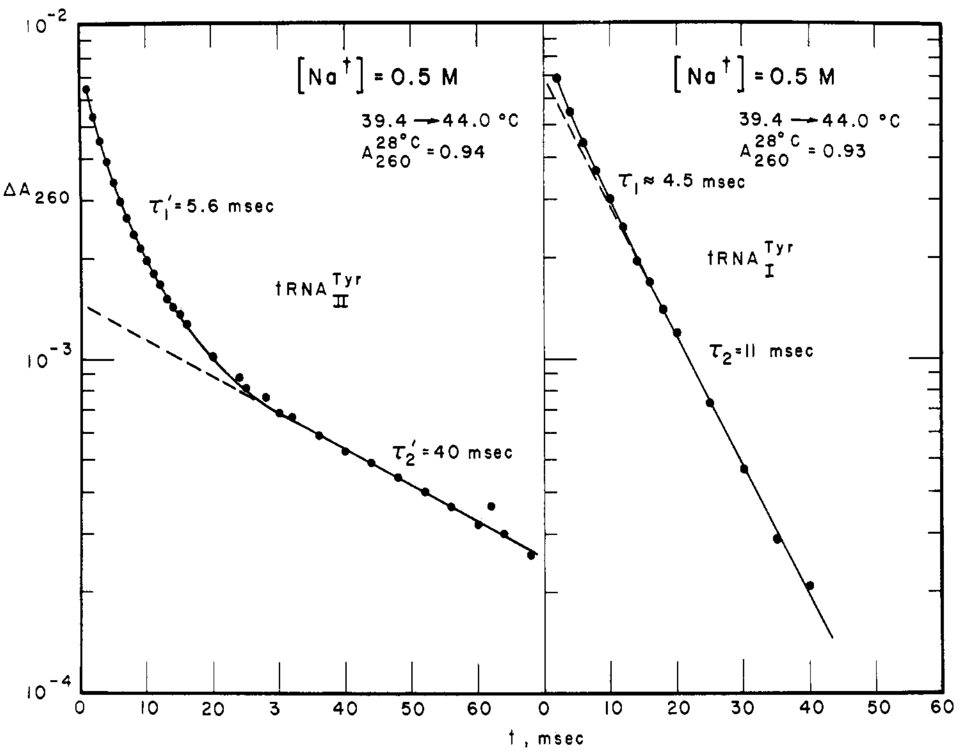

FIGURE 8: Semi-logarithmic analysis of the relaxation signals of tRNA$_{\text{I}}^{\text{Tyr}}$ and tRNA$_{\text{II}}^{\text{Tyr}}$ in 0.5 PCEP at identical conditions.

tRNA$_{\text{I}}^{\text{Tyr}}$ and tRNA$_{\text{II}}^{\text{Tyr}}$. The relaxation τ_2' for tRNA$_{\text{II}}^{\text{Tyr}}$ is considerably slower than the dominant tRNA$_{\text{I}}^{\text{Tyr}}$ relaxation (τ_2), and has a larger temperature dependence below the T_m for the early transition. This indicates that the activation energy for structure formation by the mechanism τ_2' in tRNA$_{\text{II}}^{\text{Tyr}}$ probably has a larger activation energy than the analogous reaction in tRNA$_{\text{I}}^{\text{Tyr}}$, although we were not able to estimate $E_{\text{act}}^{\text{R}}$ for τ_2' because of the small signal amplitude and very slow rate. *These properties of τ_2' are what one would expect on the basis of the more stable extra structure in tRNA$_{II}^{Tyr}$: its bonding blocks formation of the native tertiary structure, slowing that reaction by increasing its activation energy.*

The relaxation τ_1', and its lack of activation energy, were a surprise to us, however. The two-relaxation pattern is analogous to tRNA$^{\text{fMet}}$ (Cole and Crothers, 1972), and indicates again that the tertiary structure can melt in two steps. Since τ_1' is fast and has little activation energy, it seems that *the extra or incorrect structure in tRNA$_{II}^{Tyr}$ blocks only one of the regions involved in tertiary structure formation.* The results also indicate, by analogy, that *the incorrect structure in tRNA$_{I}^{Tyr}$ blocks both of these regions.*

The Kinetics of Dissociating the Native Tertiary Structure Is Very Similar for the Two tRNAs. This is shown by Figure 10, comparing the measured relaxation times for tRNA$_{\text{I}}^{\text{Tyr}}$ and tRNA$_{\text{II}}^{\text{Tyr}}$ above the T_m in 0.12 M Na$^+$. Only a single relaxation time can be reliably measured in this range for tRNA$_{\text{I}}^{\text{Tyr}}$, while for tRNA$_{\text{II}}^{\text{Tyr}}$, τ_1' and τ_2' coalesce together to give a single relaxation, virtually identical with τ for tRNA$_{\text{I}}^{\text{Tyr}}$. At the end of the transition the two tRNAs diverge again because of the extra transition of tRNA$_{\text{II}}^{\text{Tyr}}$. Since the rate of dissociating the tertiary structure is the same in both cases, *we find no evidence that the tertiary structure is different in tRNA$_{I}^{Tyr}$ and tRNA$_{II}^{Tyr}$.*

The Thermal Difference Spectrum of the Relaxation Signal Indicates Melting of a Region Less G·C Rich than the Total tRNA. Figure 11 shows the wavelength dependence of the amplitude of the relaxation signal for the two tRNAs in a temperature region where both show only a single decay time. According to the parameters of Fresco *et al.* (1963), the region melting is approximately 50% G·C pairs. Since the acceptor

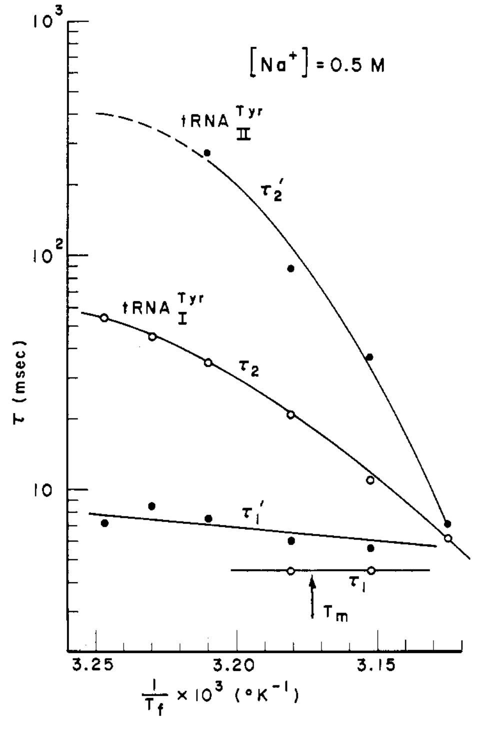

FIGURE 9: Relaxation times of tRNA$_{\text{I}}^{\text{Tyr}}$ (O-O-O) and tRNA$_{\text{II}}^{\text{Tyr}}$ (●-●-●) determined at 266 nm in 0.5 PCEP are plotted *vs.* reciprocal temperatures. The temperature jump was 4.6° and T_f is the final temperature after temperature jump. The T_m value of the thermal transition is indicated by an arrow on the temperature axis.

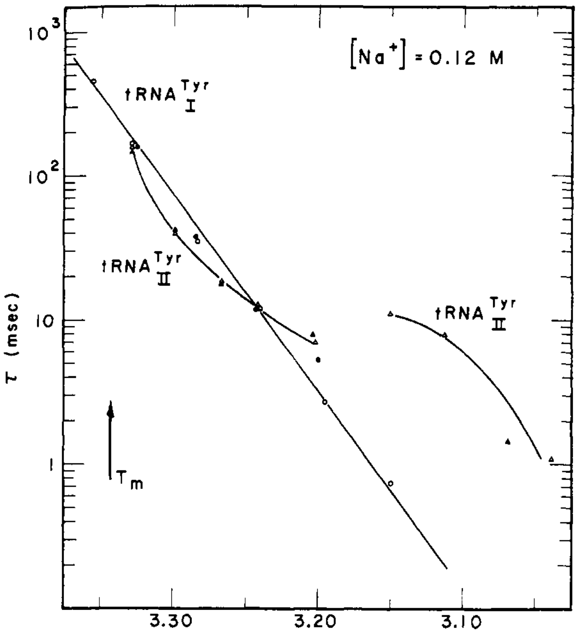

FIGURE 10: Relaxation times of tRNA$_I^{Tyr}$ (○-○-○ and ●-●-●) and tRNA$_{II}^{Tyr}$ (△-△-△ and ▲-▲-▲) determined at 266 (open circles and triangles) and 335 nm (filled circles and triangles) in 0.12 PCEP are plotted *vs.* reciprocal temperatures. The temperature jump was 4.6° and T_f is the final temperature after the temperature jump. The T_m value of the thermal transition is indicated by an arrow on the temperature axis.

stem contains 1 A·U and 6 G·C pairs, the spectroscopic equivalent of 4 or 5 A·U pairs from some other source would have to melt with the stem in order to explain the thermal difference spectrum. This seems impossible in view of the size of the optical change and the measured dissociation heat (Table I), and we conclude, as with tRNA^{fMet}, that the acceptor stem does not melt in the early transition.

Discussion

General Implications. We will not repeat in detail the arguments developed for tRNA^{fMet} by Cole and Crothers (1972), leading to the general conclusion that the early melting transition involves loss of tertiary structure, and possibly also melting of the dihydrouridine helix. The same statement applies to tRNA^{Tyr}. The important feature of the present results is the difference between the early transition of tRNA$_I^{Tyr}$ and tRNA$_{II}^{Tyr}$, and the clear contrast with the kinetic behavior of tRNA^{fMet}. For both of the tyrosine-specific tRNAs, the relatively slow rate of reforming the native structure from the partly melted intermediate, and the substantial activation energy for this process, indicate that form II (the product of the early melting transition) contains some incorrect (noncloverleaf) bonding that is not compatible with the native structure.

Several observations indicate that this incorrect bonding is stronger in tRNA$_{II}^{Tyr}$ than in tRNA$_I^{Tyr}$. The rate of reforming the native structure in tRNA$_{II}^{Tyr}$ is slower than for tRNA$_I^{Tyr}$, implying that a smaller fraction of the tRNA$_{II}^{Tyr}$ molecules are in a reactive state, assumed to be that with the incorrect structure broken. Furthermore, the activation energy, which should reflect the heat required to break up the incorrect structure, appears to be larger for tRNA$_{II}^{Tyr}$ than for tRNA$_I^{Tyr}$. Finally, the breakup of the incorrect structure

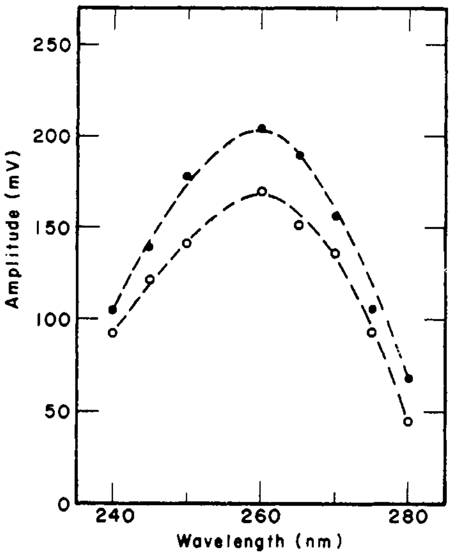

FIGURE 11: Difference spectra of tRNA$_I^{Tyr}$ (○-○-○) and tRNA$_{II}^{Tyr}$ (●-●-●) in 0.174 PCEP. Oscilloscope traces of relaxation signals for a temperature jump from 28.1 to 39.1° at wavelengths indicated were analyzed. The total amplitudes (in millivolts) corresponding to the single relaxation effect cf each wavelength are plotted against wavelength. Sample concentration (absorbance measured at 26°): tRNA$_I^{Tyr}$, 0.891A_{260}/ml. tRNA$_{II}^{Tyr}$, 0.950 A_{260}/ml. The relaxation time measured at all wavelengths was 10 ± 1 msec for tRNA$_I^{Tyr}$ and 7 ± 1 msec for tRNA$_{II}^{Tyr}$.

in tRNA$_{II}^{Tyr}$ can be associated with the extra melting transition observed for that species. The analogous reaction for tRNA$_I^{Tyr}$ must be assigned to a process at lower temperature, in the early transition; hence the incorrect structure for tRNA$_I^{Tyr}$ is again concluded to be less stable than for tRNA$_{II}^{Tyr}$.

What Is the Structural Basis for the Incorrect Bonding? The experimental results narrow greatly the possibilities for the noncloverleaf bonding. It must involve the sequence region where the two tRNAs are different, and does not include the anticodon helix, the acceptor stem, or the TψC helix, since these melt in the high-temperature transition. The two tRNAs differ in the sequence region between the anticodon helix and TψC helix, sometimes called the extra arm, miniloop, or variable-length region. In the standard structure given in Figure 1 this region is shown bonded in a helix of 3 base pairs, with an unbonded loop of three nucleotides. Recent experiments on model oligonucleotides (Gralla and Crothers, 1972) make clear that after the tertiary structure has melted, this helix is unstable and the entire miniloop should be available for bonding. Even in the native structure, this part of the molecule is not as strongly bonded as other cloverleaf helix regions, as shown by the measurements of oligonucleotide binding reported by Uhlenbeck (1972).

The model we propose for the incorrect bonding, formed *after* loss of tertiary structure, is shown in Figure 12. The miniloop region bonds to 4 nucleotides in the anticodon loop in tRNA$_{II}^{Tyr}$, and to 4 nucleotides in the TψC loop in tRNA$_I^{Tyr}$. The difference in stability could be explained in either of two ways: (1) because the four-base-pair helix in tRNA$_{II}^{Tyr}$ is stacked without interruption on the anticodon helix, while the four pairs in tRNA$_I^{Tyr}$ form a separate helix; or (2) because the anticodon loop has a special affinity for bonding oligonucleotides, a property not characteristic of the TψC loop. Uhlenbeck's (1972) experiments, as well as those of Eisinger *et al.* (1971), indicate that the anticodon loop does have special bonding properties, but since the TψC loop is inaccessible in native tRNA there is no present information about its intrinsic affinity for complementary oligonucleotides.

Another feature of interest in the results is the indication that the incorrect structure in tRNA$_{\text{II}}^{\text{Tyr}}$ blocks only one of the regions of interaction in the tertiary structure, while the incorrect structure in tRNA$_{\text{I}}^{\text{Tyr}}$ blocks them both. Since the anticodon loop is available for binding oligonucleotides in native tRNA (Uhlenbeck, 1972), it must be the involvement of the miniloop that inhibits formation of tertiary structure in tRNA$_{\text{II}}^{\text{Tyr}}$. We see two possible ways that bonding of the miniloop to the anticodon could block tertiary structure formation: (1) nucleotides in the miniloop are involved in base pairing in the tertiary structure, and hence the bond to the anticodon loop must be broken before the native structure can be formed, or (2) bonding of the miniloop to the anticodon is not sterically compatible with the native structure, even though the nucleotides in the miniloop are not actually involved in pairing in the native structure. We consider that the evidence is not yet sufficient to distinguish these two possibilities.

Whereas bonding of the miniloop to the anticodon blocks one of the steps in the formation of tertiary structure, bonding of the miniloop to the TψC loop seems to inhibit both steps. This is consistent with the view that the TψC loop is actively involved in tertiary bonding, whereas the anticodon loop is not. One conclusion that these considerations imply is that *bonding of the miniloop to the anticodon does not block tertiary structure formation that involves the TψC loop.*

What Is the Detailed Kinetic Mechanism? The uncertainties discussed in connection with the kinetic mechanism of the early transition in tRNA$^{\text{fMet}}$ apply as well to the present cases. It is possible to write several mechanisms that satisfy the kinetic observations, and these cannot be distinguished unambiguously. There must again be (at least) two regions of the tertiary structure, but the order in which these can or must melt is uncertain. For the sake of consistency we present formal mechanisms that correspond to that given for tRNA$^{\text{fMet}}$ (Cole and Crothers, 1972): the two regions of the tertiary structure can melt separately, giving two reaction paths to produce a cloverleaf structure. In tRNA$^{\text{Tyr}}$, however, the cloverleaf CL (with the dihydrouridine loop possibly melted) can react further to produce an incorrect structure Z

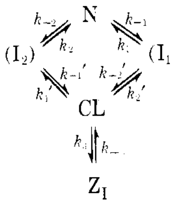

tRNA$_\text{I}^{\text{Tyr}}$

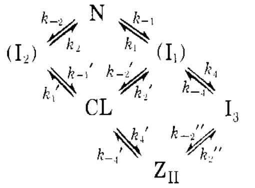

tRNA$_{\text{II}}^{\text{Tyr}}$

In these reaction schemes, species in parentheses are steady-state intermediates, included to maintain the general reaction framework proposed for tRNA$^{\text{fMet}}$. The rate constants k_i, k_i', and k_i'' (or k_{-i}, k_{-i}, k_{-i}'') refer to formation (or dissociation) of bonded structure in region i of the molecule. The difference in the two tRNA$^{\text{Tyr}}$ mechanisms is that in tRNA$_{\text{II}}^{\text{Tyr}}$, formation of region 2 of the tertiary structure (rate constants k_2, k_2', and k_2'') is not blocked by the incorrect structure (structural region 4), whereas the incorrect structure in tRNA$_{\text{I}}^{\text{Tyr}}$ (structural region 3) blocks *both* the tertiary structural regions 1 and 2.

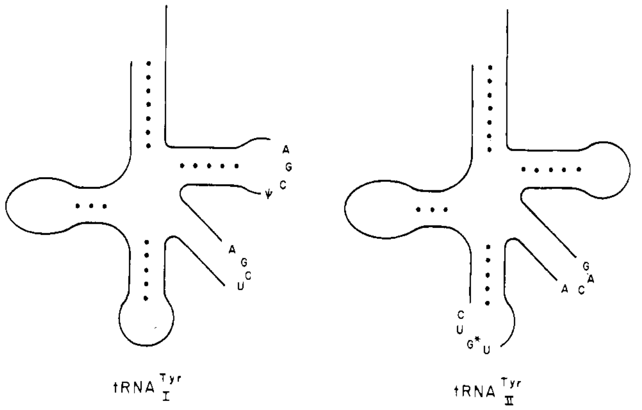

FIGURE 12: Proposed incorrect bonding for tRNA$_{\text{I}}^{\text{Tyr}}$ and tRNA$_{\text{II}}^{\text{Tyr}}$ after the melting of tertiary structure. In each case, we show only the complementary sections of the sequence that produce the incorrect bonding.

The reaction scheme for tRNA$_{\text{I}}^{\text{Tyr}}$ predicts two detectable relaxation times: the dominant relaxation is conversion between N and Z$_\text{I}$, or, at higher temperatures, a mixture of Z$_\text{I}$ and CL. The other relaxation is the faster conversion of CL and Z$_\text{I}$. The reaction scheme for tRNA$_{\text{II}}^{\text{Tyr}}$ predicts three relaxations: the conversions between Z$_{\text{II}}$, I$_3$, and N supply the two relaxations in the early transition; the reaction $\text{Z}_{\text{II}} \rightleftarrows \text{I}_3$ is rapid and has little activation energy (involving region 2 of the tertiary structure), while $(\text{I}_3 + \text{Z}_{\text{II}}) \rightleftarrows \text{N}$ is slow and has a large activation energy because of k_{-4} and k_{-4}'. The third relaxation, seen in the "extra" transition, is $\text{Z}_{\text{II}} \rightleftarrows \text{CL}$. Since we consider these mechanisms illustrative rather than definitive, algebraic expressions for the relaxation times will not be presented.

Is the Conformational Difference between tRNA$_I^{Tyr}$ and tRNA$_{II}^{Tyr}$ Functionally Significant? The answer to this question is, of course, not known at present. If the tertiary structure of tRNA unfolds during its role in protein synthesis, then the two tRNAs have different conformational states available to them. In this way the variable-length region of tRNA could serve to modulate conformation in a functionally important way. Only those tRNAs that have more than a few nucleotides in that section of the sequence could function in this manner, however.

References

Cole, P. E., and Crothers, D. M. (1972), *Biochemistry 11*, 4368.

Cole, P. E., Yang, S. K., and Crothers, D. M. (1972), *Biochemistry 11*, 4358.

Eisinger, J., Feuer, B., and Yamane, T. (1971), *Nature (London), New Biol. 231*, 126.

Fresco, J. R., Klotz, L. C., and Richards, E. G. (1963), *Cold Spring Harbor Symp. Quant. Biol. 28*, 83.

Goodman, H. M., Abelson, J., Landy, A., Brenner, S., and Smith, J. D. (1968), *Nature (London) 217*, 1019.

Gralla, J., and Crothers, D. M. (1972), *J. Mol. Biol.* (in press).

RajBandary, U. L., Chang, S. H., Gross, H. J., Harada, F., Kimura, F., and Nishimura, S. (1969), *Fed. Proc., Fed. Amer. Soc. Exp. Biol. 28*, 409.

Uhlenbeck, O. C. (1972), *J. Mol. Biol. 65*, 25.

Yang, S. K. (1972), Ph.D. Thesis, Yale University.

Yang, S. K., Söll, D. G., and Crothers, D. M. (1972), *Biochemistry 11*, 2311.